Hydrogen Bonding

Deutsche Ausgabe: DOI: 10.1002/ange.201603319
Internationale Ausgabe: DOI: 10.1002/anie.201603319

Hydrogen-Bond Cooperativity in Formamide$_2$–Water: A Model for Water-Mediated Interactions

*Susana Blanco, Pablo Pinacho, and Juan Carlos López**

Abstract: *The rotational spectrum of formamide$_2$–H_2O formed in a supersonic jet has been characterized by Fourier-transform microwave spectroscopy. This adduct provides a simple model of water-mediated interaction involving the amide linkages, as occur in protein folding or amide-association processes, showing the interplay between self-association and solvation. Mono-substituted ^{13}C, ^{15}N, ^{18}O, and ^{2}H isotopologues have been observed and their data used to investigate the structure. The adduct forms an almost planar three-body sequential cycle. The two formamide molecules link on one side through an N−H⋯O hydrogen bond and on the other side through a water-mediated interaction with the formation of C=O⋯H−O and O⋯H−N hydrogen bonds. The analysis of the quadrupole coupling effects of two ^{14}N-nuclei reveals the subtle inductive forces associated to cooperative hydrogen bonding. These forces are involved in the changes in the C=O and C−N bond lengths with respect to pure formamide.*

Hydrogen bonding (HB) is responsible for most of the inter- and intramolecular interactions that underpin protein folding, protein structure, biological activity. and molecular recognition.[1,2] The hydrogen-bonding interactions N−H⋯O=C involving the amide linkages dominate in the hydrophobic core of the proteins.[3] However, the mediation of water to form C=O⋯H−N contacts has been reported to occur in proteins with turn structures as far as the turns are located near the protein surface where they are exposed to interactions with water.[4] Water mediation has been also proposed to be important in the nucleation process of protein folding.[5] Another point of interest concerning hydrogen bonding in protein structures is the stabilization due to cooperative forces.[2,6,7] Cooperativity has contributions from entropy, owing to the restrictions of internal motions, as well as from inductive polarization of the amide groups, not yet well established owing to the small amount of experimental information on it.[8,9] The role of water to enhance, or not, hydrogen bonding cooperativity in those systems is still an open question.

Direct structural investigations of isolated clusters of molecules modelling amide–water, amide–amide, and amide–amide water-mediated interactions are important to better understand amide-association processes showing the interplay between self-association and solvation. Under the isolated conditions of supersonic jets, clusters of molecules of different sizes can be formed in a controlled way. When jets are coupled to rotationally resolving techniques, such as microwave spectroscopy, accurate structural information can be obtained. Different examples of investigations on isolated hydrated amide clusters performed in supersonic jets by microwave spectroscopy can be found in the literature.[9–16] These works, in particular the detailed investigation of the structures of formamide–$(H_2O)_n$ ($n = 1,2$)[11] (see Figure 1), have led to the observation of the conformers build from the different docking sites of formamide and some of the structural signatures of the cooperative hydrogen-bonding effects. Herein we have undertaken the study of one of the simplest systems modelling amide–amide and amide–amide water-mediated interactions, the complex formed by two molecules of formamide and one water molecule (f$_2$w, see Figure 1). We have payed special attention to accurately determine its structure and the nuclear quadrupole coupling hyperfine constants of the two ^{14}N nuclei to search for the subtle signatures of cooperative effects, particularly those which cause the inductive polarization of the amide group.

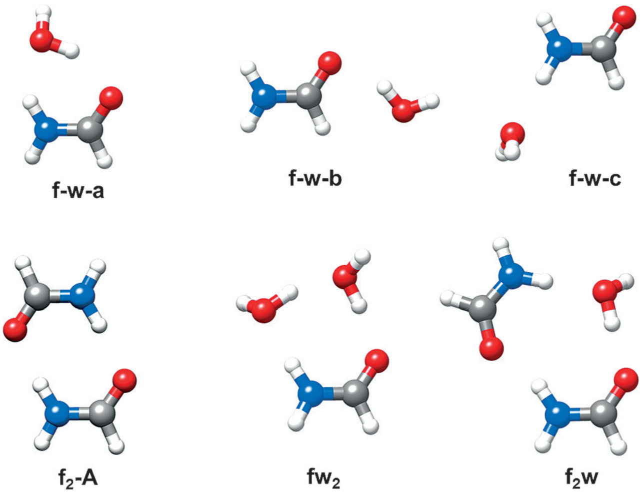

Figure 1. Adducts of formamide and water. The structures of formamide–H_2O (f-w-a, f-w-b, f-w-c),[11] formamide$_2$,[17] formamide–$(H_2O)_2$ (fw$_2$),[11] and formamide$_2$–H_2O (f$_2$w; this work). N blue, O red, H white.

We recorded the microwave spectrum of formamide–water complexes using the experimental setup described later. Once having dropped all signals with known frequencies,[11] several groups of unassigned lines appeared to show

---

[*] Prof. S. Blanco, P. Pinacho, Prof. J. C. López
Departamento de Química Física y Química Inorgánica, Facultad de Ciencias
Universidad de Valladolid
47011 Valladolid (Spain)
E-mail: jclopez@qf.uva.es

Supporting information and the ORCID identification number(s) for the author(s) of this article can be found under http://dx.doi.org/10.1002/anie.201603319.

the complicated quadrupole coupling hyperfine structure (hfs) characteristic of species having two ^{14}N nuclei (see Figure 2).[18] This hfs results from the interaction of the nuclear quadrupole moment of the ^{14}N-nuclei ($\mathbf{I}=1$), eQ, with the electric field gradient, q, at the site of the N nuclei. The corresponding spectroscopic constants, $\chi_{\alpha\beta}$ ($\alpha,\beta=a,b,c$), are the elements of the nuclear quadrupole coupling tensor, set up in the inertial principal axis system representation, and are directly related to the electric field gradient at the nitrogen nuclei ($\chi_{\alpha\beta}=eQq_{\alpha\beta}$).

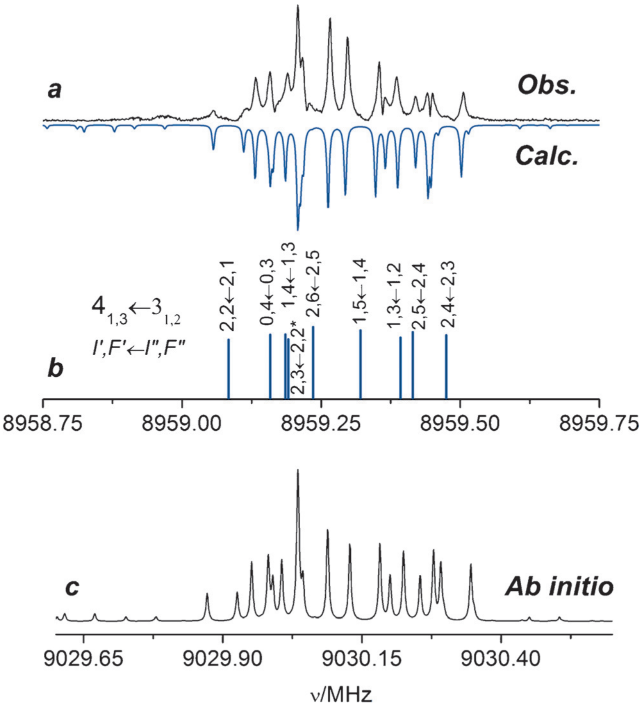

Figure 2. The transition observed around 8959.2 MHz shows the characteristic hyperfine structure of two ^{14}N nuclei, complicated by the Doppler doubling (54 kHz). a) the observed (upwards) and calculated (downwards) spectrum for the $4_{1,3}\leftarrow 3_{1,2}$. b) Assignment of the hyperfine components with the quantum numbers J, K_{-1}, K_{+1}, I, F (coupled basis set (I_1 I_2 I J F), $I_1+I_2=I$, $I+J=F$) c) Ab initio prediction for conformer f$_2$w centered at 9029.2 MHz with a hyperfine structure comparable to that observed experimentally.

To identify these new lines we considered the spectroscopic constants predicted at the MP2/6–311++g(2d,p) level for the stable forms of formamide dimers[17] (f$_2$) and formamide$_2$-water (f$_2$w) adducts (see Supporting Information Table S1, S2 and Figures S1 and S2). The best match in both frequency and quadrupole coupling patterns corresponds to the predicted most stable f$_2$w conformer as can be seen in Figure 2. The most stable species of formamide dimer, f$_2$-A, (Figure 1), expected to be dominant by far in the gas phase, has an inversion center, and thus has no microwave spectrum. The assignment of the quadrupole coupling patterns for several R-branch μ_a-type transitions lead to the complete measurement of the μ_a- and μ_b-type R-branch spectra. The μ_c-type spectrum was not observed. The rotational parameters determined from the analysis of the spectrum are compared in Table 1 with the ab initio constants for the most stable form of f$_2$w complex.

Table 1: Rotational parameters obtained from the analysis of the spectrum of the observed formamide$_2$–water adduct.

Fitted Parameters[a]	Exp. value[b]	Ab initio f2w
A/MHz	2769.21575(56)	2725
B/MHz	1232.34734(17)	1244
C/MHz	854.50629(10)	860
P_{cc}/uÅ^2	0.582754(80)	2.0317
$^{14}N_3$ χ_{aa}/MHz	1.0671(44)	1.09
$^{14}N_3$ χ_{bb}/MHz	1.9087(86)	2.05
$^{14}N_3\chi_{cc}$/MHz	−2.9757(86)	−3.14
$^{14}N_9$ χ_{aa}/MHz	1.2692(37)	1.20
$^{14}N_9$ χ_{bb}/MHz	1.7260(83)	1.80
$^{14}N_9$ χ_{cc}/MHz	−2.9952(83)	−3.00
N	206	
σ/kHz	1.5	

[a] A, B, and C are the rotational constants. χ_{aa}, χ_{bb} and χ_{cc} are the quadrupole coupling constants for $^{14}N_3$ and $^{14}N_9$ nuclei (see Figure 3). N is the number of quadrupole hyperfine components fitted. σ is the rms deviations of the fit, the value 1.5 kHz is within the estimated accuracy of frequency measurements. $P_{cc}=(I_a+I_b-I_c)/2=\left(\sum_i m_i c_i^2\right)/2$, is a planar moment of inertia (conversion factor 505679.1 MHz uÅ^{-2}.
[b] Standard error is given in parentheses in units of the last digit.

Well stablished structural-determination methods beyond the simple conformation identification based on the comparison of the observed and ab initio rotational parameters use data from the spectra of the parent and isotopically substituted species. To exploit those methods, the spectra of the monosubstituted species $^{15}N_3$, $^{15}N_9$, $^{15}N_3$–$^{15}N_9$, $^{13}C_2$, $^{13}C_8$, $^{18}O_{14}$, and $^2H_{13}$ (see Figure 3 for labeling) were measured. The observation of the $^2H_{15}$ spectrum was not possible because of overlapping with other spectra. The complete sets of determined parameters, details of the analysis and observed frequencies are collected in the Supporting Information, Table S3–S12.

The nearly identical values of the B rotational constant (see Table 1 and S4) for the parent and $^{18}O_{14}$ species indicates that the water oxygen atom lies along the b inertial axis. The planar moment of inertia, P_{cc}, which gives a measure of the mass extension out of the ab inertial plane, takes a nearly constant value (around 0.58 uÅ^2, see Table 1 and S4) for all isotopologues. Therefore, a planar atom skeleton coincident with the ab inertial plane is concluded. Only the non-bonded water hydrogen atom, H$_{15}$, is out of this plane.

The Kraitchman, r_s, substitution method,[19] exploits changes in the moments of inertia upon mono-isotopic substitution to provide the absolute values of the atom coordinates of the substituted atoms in the principal inertial axis frame. This purely experimental approach allows to directly locating the different atoms of a molecule but it poses limitations for atoms located near the three principal axes. An alternative way to exploiting multi-isotopic information is to obtain the bond distances and angles from a least squares fit of all of the available rotational parameters[20] to determine a total or partial effective ground state, r_0, structure. The r_0 principal inertial axis coordinates or those taken from

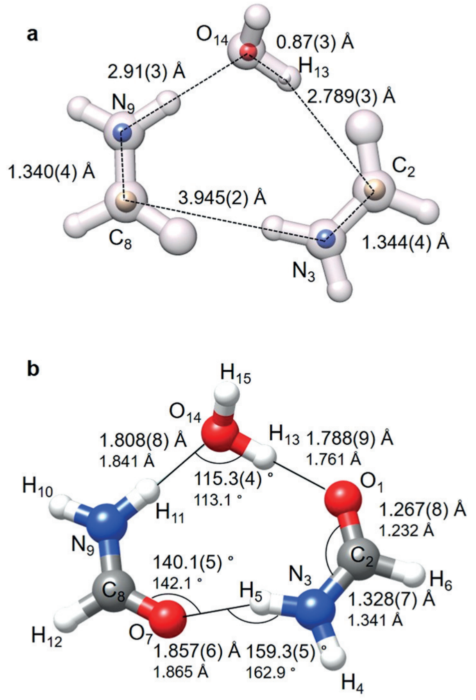

Figure 3. a) The experimental r_s position of the isotopically substituted atoms of formamide$_2$–H$_2$O with the ab initio structure. The r_s interatomic distances are also given. b) The experimental r_0 bond lengths and angles of formamide$_2$–H$_2$O (upper values) and the ab initio MP2/6-311++G(2d,p) predictions (lower values).

ab initio computations can be used to assign the coordinate signs to the r_s coordinates allowing for the eventual unambiguous identification of a given cluster.

The results of the application of the r_s and r_0 methods are summarized in Figure 3 where they show a good consistency with the ab initio data. The r_s coordinates are collected in Table S13 of the Supporting Information. The r_0 data and the details of the calculations are collected in Table S14 were they are compared to those of ab initio calculations. The experimental structure (see Figure 3) reflects that the two formamide subunits close a sequential cycle with water through three hydrogen bonds, C=O···H–N, N–H···OH, and O–H···O=C. This is possible thanks to the hydrogen bond donor/acceptor double character of both water and formamide molecules. The hydrogen bond lengths indicate that the dominant interaction is O–H···O=C as reported for related systems[11,12] and in agreement with the observed preference of water to interact with this group in globular proteins.[1]

The so called σ-bond cooperativity is associated to chains or cycles of hydrogen bonds between groups acting simultaneously as donor and acceptor.[2] Sequential cycles are characterized by a shortening of the hydrogen bond distances and an increment of hydrogen bond energy as the members of the cycle increase. The hydrogen bond distances related to the O–H···O=C and N–H···O bonds of f$_2$w are shorter that those of related sequential cycles such as formamide–(H$_2$O)$_n$ (n = 1,2),[11] the water dimers[21] and trimers,[22] or formamide dimer in liquid phase[23] (see Table S16). The f$_2$w bond lengths are only comparable to those of the three body adduct formamide–(H$_2$O)$_2$. Similar conclusions can be reached by considering the calculated dissociation energies (Table S16).

Resonance-assisted hydrogen bonding (RAHB)[8] or π-cooperative bonding was first pointed out to occur in the case of the peptide linkage[2,24] from studies of the crystal structures of small amides. The main effect of this cooperativity in the structure of formamide is the C=O bond lengthens and the C–N peptide bond shortens owing to the formation of open and closed dimers. This effect not yet reported in the gas phase from rotational spectroscopy has been observed in this work as illustrated in Scheme 1 where the r_0(C–N) and r_0(C=O) distances for formamide and f$_2$w (see Table S14–S16) are shown.

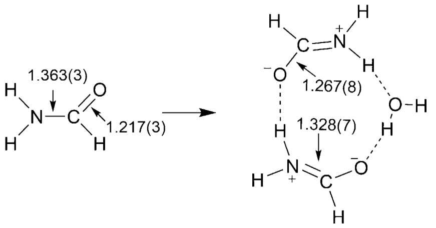

Scheme 1. Cooperative hydrogen-bond inductive effects in the formation of f$_2$w are evidenced by the C=O bond length increase and C–N bond length decrease.[2].

The ^{14}N quadruple coupling constants are expected to be very sensitive to the small changes in the electronic environment at these nuclei produced by inductive cooperative effects. A complete picture of the electric field gradient can only be obtained from the complete determination of the quadrupole coupling tensor. In the present case, only the diagonal elements have been determined, but we can still extract information from it. In pure formamide, the c inertial axis, perpendicular to the plane of the molecule, is parallel to one of the principal ^{14}N quadrupole coupling axis, say z ($\chi_{cc} = \chi_{zz}$). Given the planarity of the skeleton of f$_2$w, its c inertial axis is almost perpendicular to the formamide molecular planes so $\chi_{cc} \approx \chi_{zz}$. This planar arrangement is common to all complexes of water and formamide studied so far.[11] As shown in Table S17 there is a progressive decrease in the value of χ_{cc} going from formamide to its microsolvated complexes. The agreement between the experimental decrements and the ab initio values, based on a static picture, allow to discard intermolecular oscillations[25] as the main cause of this effect. This correlation in the values of χ_{cc} indicates that the electronic environment of the N atom of formamide is altered to some extent by the formation of one or successive hydrogen bonds.

The electric field gradient giving rise to nuclear quadrupole coupling in molecules has often been attributed to the unequal filling of the p orbitals of the valence shell of the coupling atoms.[18] According to this, the ^{14}N χ_{zz} constants can be related to the unbalanced 2p$_z$ electronic charge $(U_p)_z = \left[(n_x - n_y)/2 - n_z\right]$ by [Eq. (1)]:

$$\chi_{zz}/eQq_{210} = -(U_p)_z \tag{1}$$

where n_α are the p_α orbital occupation numbers and q_{210} the electric field gradient associated to a 2p electron in an isolated atom ($eQq_{210} \approx -10$ MHz for N). This definition of $(U_p)_z$ is such that its positive or negative values correspond, respectively to electron deficit or excess along the z reference axis.[18] The values of χ_{zz}/eQq_{210} obtained from the experimental χ_{cc} values are plotted in Figure 4 versus those calculated using the natural atomic orbital populations from a natural bond orbital (NBO) analysis.[26] Despite the approximations, they show and excellent agreement. According to the definition of $(U_p)_z$, the electron density excess along the z axis in formamide decreases progressively in the complexes as the size of the cycle increases. There is a small decrease even for f-w-b ($-(U_p)_z = 0.36$), where the NH_2 is not involved in hydrogen bonding. This illustrates how the amide group is progressively polarized due to inductive effects, which increase with the number of cooperating hydrogen bonds.

	f	f-w-a	fw$_2$	f$_2$w-N$_3$	f$_2$w-N$_9$	f-w-b
χ_{cc}/eQq_{210}	0.385	0.337	0.308	0.298	0.300	0.360
$-(U_p)_z$	0.382	0.330	0.299	0.299	0.301	0.364
η_D	0.042	0.224	0.348	0.346	0.384	0.038

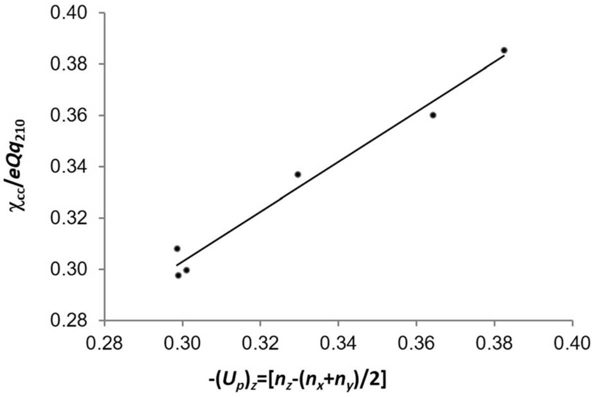

Figure 4. Plot of the values (see top table) of the quantity χ_{cc}/eQq_{210} versus the unbalanced 2 p_z electronic charge $(U_p)_z$ obtained from a NBO analysis of formamide, formamide–H_2O (f-w-a), formamide–$(H_2O)_2$ (fw$_2$), and formamide$_2$–H_2O (f$_2$w). The slope of the line is 0.96.

The asymmetry parameter $\eta_D = |(\chi_{yy} - \chi_{xx})/\chi_{zz}|$, which takes values between 0 and 1, measures the deviation of the charge distribution from axial symmetry ($\eta_D = 0$). The ab initio values of η_D (see Figure 4 and Table S17) show noticeable changes from formamide and f-w-b, which are predicted to have an almost symmetric distribution of charge ($\eta_D \approx 0.04$), to formamide–H_2O ($\eta_D \approx 0.22$) and for three body clusters ($\eta_D \approx 0.35$–0.38). The NBO analysis gives additional information about charge transfer in these clusters and allows us to give an interpretation of the steady enlargement of the C=O bond and decrease of C–N bond of formamide in the sequential cycle clusters based on the progressive increase of electron density on the carbonyl group π* antibonding orbital and the progressive decrease of the small electron density in the C–N bond σ* natural orbital, respectively.

In conclusion the adduct formamide$_2$–H_2O illustrates the way in which water may act as a mediator in amide-association processes, such as those of protein folding. The structure of the complex reflects clearly the effects of hydrogen bonding σ- and π-cooperativity.[2] The hydrogen bond lengths are shorter than in the related sequential cycles. The heavy-atom skeleton adopts a cyclic planar structure showing a directionality that may be important in the process of protein folding. The C–N and C=O bonds of formamide subunits became shorter or larger, respectively, upon formation of the complex. One of the most interesting aspects of this research is the confirmation that the quadrupole coupling interaction can be taken as a probe for the inductive processes accompanying cooperativity which alter the electronic structure of the amide group upon polarization. Another remarkable result concerning cooperative effects, is the similarity observed in the structural and quadrupole coupling data in the three body adducts formamide$_2$–H_2O and formamide–$(H_2O)_2$. This suggests that the acid/base properties of formamide and water are not very different. In this way, if formamide–$(H_2O)_2$ is considered as a microsolvated formamide adduct, formamide$_2$–H_2O could also be seen as a microsolvated water adduct with formamide being the solvent in this case. Finally this work shows that water is able to enhance cooperative hydrogen-bonding effects which can be important when water mediates in the nucleation process of protein folding.

Experimental Section

Commercial samples of the parent and isotopic species of formamide and water were used. The molecular-beam Fourier transform microwave spectrometer (MB-FTMW), described elsewhere,[27] was operated in the frequency range 5–13 GHz. The supersonic jet was generated by expansion of a gas mixture He–Ne at backing pressures of about 12 bar through a small (0.9 mm diameter) pulsed heatable nozzle.[28] Formamide (b.p. 210 °C) was placed in a nozzle at about 50 °C and water in a reservoir inserted in the gas line just before the nozzle. Short (typ. 0.3 μs, 10–300 mW) microwave pulses were used for polarization purposes. Typically, a ca. 400 μs-length time domain spectrum was recorded in 40–100 ns intervals and converted into the frequency domain by a fast Fourier transformation. Due to the collinear arrangement of the jet and resonator axis each rotational transition splits in two Doppler components so the resonant frequencies are taken as the arithmetic mean of both components. Frequency accuracy is better than 3 kHz. Ab initio calculations (MP2/6-311++G(2d,p)) were done using the G09 package.[29] The counterpoise procedure[30] was used to calculate the dissociation energies. NBO analysis were also done using NBO 5.9.[31]

Acknowledgements

We acknowledge the Ministerio de Economía y competitividad (Grant CTQ2013-40717-P) and the Junta de Castilla y León (Grant VA334U14) for financial support.

Keywords: cooperative effects · hydrogen bonds · formamide · rotational spectroscopy · water-mediated interactions

How to cite: *Angew. Chem. Int. Ed.* **2016**, *55*, 9331–9335
Angew. Chem. **2016**, *128*, 9477–9481

[1] E. N. Baker, R. E. Hubbard, *Prog. Biophys. Mol. Biol.* **1984**, *44*, 97 – 179.
[2] G. A. Jeffrey, *An Introduction to Hydrogen Bonding*, Oxford University Press, Oxford, **1997**.
[3] C. M. Venkatachalam, *Biopolymers* **1968**, *6*, 1425 – 1436.
[4] I. D. Kuntz, *J. Am. Chem. Soc.* **1972**, *94*, 4009 – 4012.
[5] S. Busch, C. D. Bruce, C. Redfield, C. D. Lorenz, S. E. McLain, *Angew. Chem. Int. Ed.* **2013**, *52*, 13091 – 13095; *Angew. Chem.* **2013**, *125*, 13329 – 13333.
[6] A. S. Mahadevi, G. N. Sastry, *Chem. Rev.* **2016**, *116*, 2775 – 2825.
[7] H. Kawai, R. Katoono, K. Nishimura, S. Matsuda, K. Fujiwara, T. Tsuji, T. Suzuki, *J. Am. Chem. Soc.* **2004**, *126*, 5034 – 5035.
[8] P. Gilli, V. Bertolasi, V. Ferretti, G. Gilli, *J. Am. Chem. Soc.* **2000**, *122*, 10405 – 10417.
[9] A. Held, D. W. Pratt, *J. Am. Chem. Soc.* **1993**, *115*, 9708 – 9717.
[10] F. J. Lovas, R. D. Suenram, G. T. Fraser, C. W. Gillies, J. Zozom, *J. Chem. Phys.* **1988**, *88*, 722 – 729.
[11] S. Blanco, J. C. López, A. Lesarri, J. L. Alonso, *J. Am. Chem. Soc.* **2006**, *128*, 12111 – 12121.
[12] J. C. López, R. Sánchez, S. Blanco, J. L. Alonso, *Phys. Chem. Chem. Phys.* **2015**, *17*, 2054 – 2066.
[13] W. Caminati, J. C. López, S. Blanco, S. Mata, J. L. Alonso, *Phys. Chem. Chem. Phys.* **2010**, *12*, 10230 – 10234.
[14] R. J. Lavrich, M. J. Tubergen, *J. Am. Chem. Soc.* **2000**, *122*, 2938 – 2943.
[15] A. Maris, P. Ottaviani, W. Caminati, *Chem. Phys. Lett.* **2002**, *360*, 155 – 160.
[16] S. Mata, V. Cortijo, W. Caminati, J. L. Alonso, M. E. Sanz, J. C. López, S. Blanco, *J. Phys. Chem. A* **2010**, *114*, 11393 – 11398.
[17] C. Colominas, F. J. Luque, M. Orozco, *J. Phys. Chem. A* **1999**, *103*, 6200 – 6208.
[18] W. Gordy, R. L. Cook, *Microwave Molecular Spectra*, Wiley, New York, **1984**.
[19] J. Kraitchman, *Am. J. Phys.* **1953**, *21*, 17 – 24.
[20] Z. Kisiel, *J. Mol. Spectrosc.* **2003**, *218*, 58 – 67.
[21] T. R. Dyke, K. M. Mack, J. S. Muenter, *J. Chem. Phys.* **1977**, *66*, 498.
[22] F. N. Keutsch, J. D. Cruzan, R. J. Saykally, *Chem. Rev.* **2003**, *103*, 2533 – 2577.
[23] E. Kálmán, I. Serke, G. Pálinkás, M. D. Zeidler, F. J. Wiesmann, H. Bertagnolli, P. Chieux, *Z. Naturforsch. A* **1983**, *38*, 231 – 236; DOI: 10.1515/zna-1983-0221.
[24] T. Ottersen, P. Svanström, G. J. T. Tiddy, P. Heimbach, U. Skoglund, *Acta Chem. Scand.* **1975**, *29a*, 939 – 944.
[25] A. C. Legon, *Faraday Discuss.* **1994**, *97*, 19.
[26] A. E. Reed, R. B. Weinstock, F. Weinhold, *J. Chem. Phys.* **1985**, *83*, 735.
[27] J. Alonso, F. J. Lorenzo, J. C. López, A. Lesarri, S. Mata, H. Dreizler, *Chem. Phys.* **1997**, *218*, 267 – 275.
[28] S. Blanco, J. C. Lopez, J. L. Alonso, P. Ottaviani, W. Caminati, *J. Chem. Phys.* **2003**, *119*, 880.
[29] Gaussian 09 (Revision E.01), M. J. Frisch, et al., Gaussian Inc., Wallingford, CT **2009**.
[30] S. F. Boys, F. Bernardi, *Mol. Phys.* **1970**, *19*, 553 – 566.
[31] E. D. Glendening, J. K. Badenhoop, A. E. Reed, J. E. Carpenter, J. A. Bohmann, C. M. Morales, F. Weinhold, *Theor. Chem. Institute*, *Univ. Wisconsin*, *Madison* **2001**.

Received: April 8, 2016